Numerical Simulation of High Specific Impulse Ion Thruster Optics*†

Yoshinori Nakayama and Paul J. Wilbur
Department of Mechanical Engineering,
Colorado State University, Fort Collins, CO 80523
970-491-8691
ynakayam@nda.ac.jp

IEPC-01-99

A high specific impulse ion thruster (HiIsp-IT) operated at a voltage of 10 kV has been studied and the problems of direct ion impingement on the accelerating grid and of production and impingement of charge-exchange ions have been considered. In order to investigate these problems and to facilitate the design of HiIsp-IT grid systems, a three-dimensional particle simulation code ("igx") that employs an energy compensation method, a simplified pre-sheath definition method, a region sharing method was developed. This code also simulates the production and subsequent motion of charge-exchange ions. Using the code, results obtained quickly using a personal computer are shown to be in good agreement with experimental data associated with: (1) crossover impingement under low-beam-current condition and (2) the star-shaped pattern of the cross section of each beamlet as it passes through the accelerating grid. It argued that the "igx" code simulation is a useful tool for rapid preliminary analysis and design of HiIsp-IT grid systems. This paper also discusses an optimization method for a grid system design represented by many parameters. It is confirmed that a genetic algorithm works efficiently in this optimization application.

Introduction

There is need for propulsion systems that operate longer, have greater total impulse capabilities and can thereby accommodate the natural trend of spacecraft missions to become more ambitious. Since the propulsion system generally does not capture its propellant in space, the propellant that can be used is limited to that loaded initially. This mission trend translates, in turn therefore, to a corresponding need for ion thrusters that will make most effective use of the propellant they carry i.e. will operate at increasingly higher specific impulses.

Generally, an ion thruster has a two- or three-grid system and operates at a net accelerating voltage of the order of 1 kV (a specific impulse near 3,000 sec.). Increasing this voltage increases specific impulse, in proportion to its square root. For the work described herein, a high specific impulse ion thruster operated at a voltage of 10 kV (hereafter called HiIsp-IT) has been studied and the problems of direct ion impingement on the accelerating grid and charge-exchange ion production and impingement have been considered. These phenomena lead to sputter erosion and sputter coating effects that pose problems because then can limit thruster lifetime as a result of wear and electrical break down, respectively.

Further, a grid-system has many design parameters (*e.g.* number of electrodes, thickness, aperture diameter, gap etc.). Because of the large number of parameters involved it seems that design of a grid system would be best accomplished using high-speed numerical analysis to guide an experimental study that would otherwise be time consuming and costly.

Much numerical simulation of ion beam optics has already been done by Whealton[1], Hayakawa[2], and others[3-6]. The OPT-code[7] developed by Ishihara and Arakawa (University of Tokyo, Japan) is a well-known code. It can be used for high-speed analysis of conventional ion thruster two- or three- grid systems, and it has typically yielded results that agree reasonably well with experimental results. However, it was obvious that the results from the simulations do not agree well with experimental data in HiIsp-IT case. It appeared that the code deficiency in this high voltage case was caused by ions drawn through a screen grid hole from the region over the web between adjacent screen holes. The inherent asymmetry associated with the effects of adjacent screen holes, which becomes important under high voltage conditions, is not adequately modeled using a two-dimensional assumption when the sheath is far upstream.

Therefore, a new high-speed simulation code ("igx") was developed. This was done when it was determined

* Presented as Paper IEPC-01-99 at the 27th International Electric Propulsion Conference, Pasadena, CA, 15-19 October, 2001.

that more accurate simulations of the ion extraction and acceleration processes than those obtained from OPT are needed for HiIsp-IT applications.
The objectives of this study are (1) development of the "igx" code to enable investigation of three-dimensional ion optics and charge-exchange ion phenomena, (2) compartive evaluation of this code with experimental data.
In addition, huge numbers of calculations are required for grid system designs characterized by many design parameters. In this study, (3) an optimization method that is useful for the grid system design is also discussed.

The "igx" Code

The "igx" code[8] simulates ion extraction through ion thruster grids in a three-dimensional, cylindrical coordinate system. In order to reduce the execution time and describe the ion motion in detail, this code integrates the following concepts and methods. Figure 1 shows the flow chart of the "igx" code.

Charge Distribution

As Fig. 1 suggests, ion motion is determined using data from node point potentials. For the first calculation loop, the potentials are determined using the LaPlace equation. The motion of ions from randomly selected points on the sheath are traced. For the first loop, the sheath is assumed to be at a flat boundary far upstream of the screen grid. The Particle-In-Cell (PIC) method is used to distribute the charge of each ion to the eight mesh points that surround it at the conclusion of each time interval used in the analysis. The charge distribution is based on the area ratio algorithm suggested in Fig. 2 applied in the r-z and z-θ planes. As this figure suggests, the charge assigned to node A is proportional to the area ratio ab/h^2.

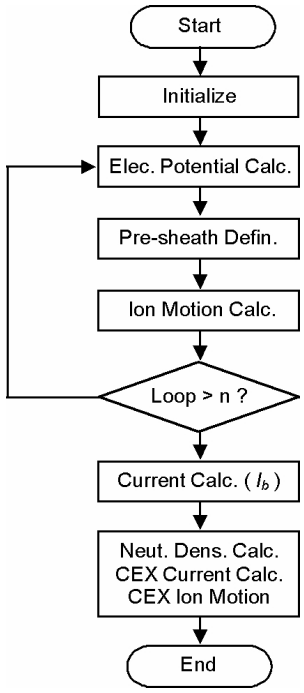

Fig. 1 Flow-chart of the "igx" code

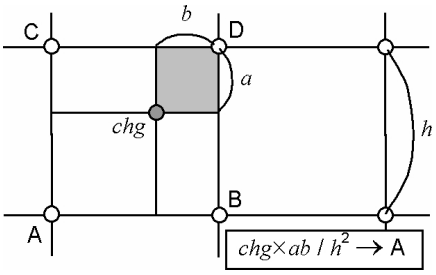

Fig. 2 Schematic of PIC method

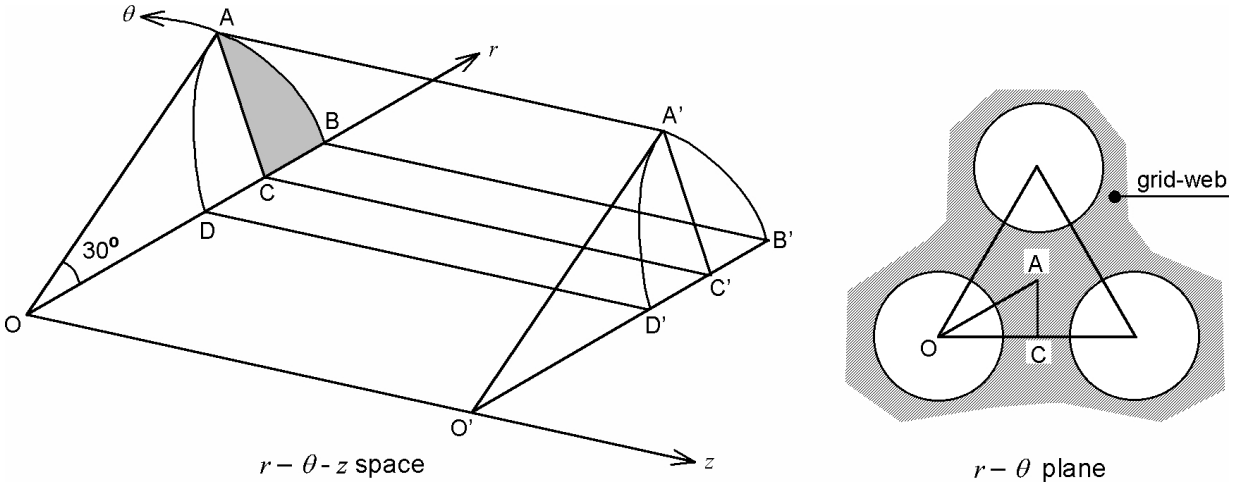

Fig. 3 Analysis space

Electrical Potential Calculation

The electrical potential (ϕ[V]) of each mesh-point within the grid-system region is calculated using Poisson's equation:

$$\nabla^2 \phi = -\frac{q}{\varepsilon} \qquad (1)$$

where q [c/m^3] and ε [F/m] are the charge density associated with a node and the dielectric constant for the medium.

The simultaneous equations associated with all of the mesh-points are solved by the successive over relaxation (SOR) method after the motions of all ions have been traced so calculation times can be reduced.

Region Sharing

Figure 3 shows the shape of the numerical space used in the code. It should be noted that point A is a unique point that is common to all three holes that surround it. In order to reduce the calculation cost, the ion motion is described in the triangular column region OAC-O'A'C' and the potential field is calculated within the cylindrical sector OAB-O'A'B'. Potentials in the column ABC-A'B'C' are determined as a mirror reflection of those in the column ADC-A'D'C' about the plane AC-A'C'.

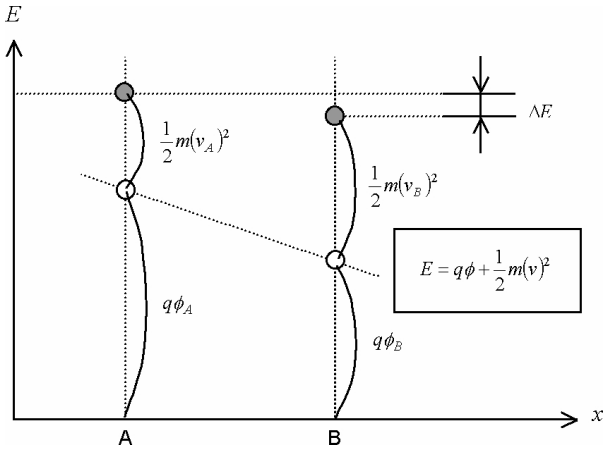

Fig. 4 Energy conservation problem

Energy Compensation

Particle motion is described in the code using the Euler method with the Courant condition applied as it is in conventional codes[9]. This is expressed in the following equations:

$$v' = v + a\Delta t\ ,\ x' = x + v\Delta t + \frac{1}{2}a\Delta t^2 \qquad (2)$$

$$\Delta v \times \Delta t \le \frac{1}{2}h\ , \qquad (3)$$

where x [m], v [m/s], t [s], a [m/s^2] and h [m] are position, velocity, time, acceleration and the length between mesh-points, respectively. The Courant condition assures a precise description of particle motion but it does not assure conservation of total energy (*i.e.* potential + kinetic energies) as given by the equation:

$$q\phi + \frac{1}{2}mv^2 = (\text{constant})\ , \qquad (4)$$

where m [kg] and ϕ [V] are mass and potential, respectively. Figure 4 illustrates the Euler method is not conservative by indicating that acceleration through the potential difference between the two points A and B typically yields an energy deficit ΔE. Figure 5 illustrates this further for the case of uniform circular motion in Cartesian coordinates using three methods of numerical analysis. When the Euler method is used (Fig. 5a) rapid divergence is obvious and when the Runga-Kutta method is used (Fig. 5b), divergence is still apparent although the Courant condition applied. A precise description of ion motion is necessary in this simulation because this code deals with ions that experience a vast energy range (over the order of magnitude range from 1 eV to 10 keV). In this simulation, therefore, compensation is applied to hold total ion energy constant at the conclusion of each

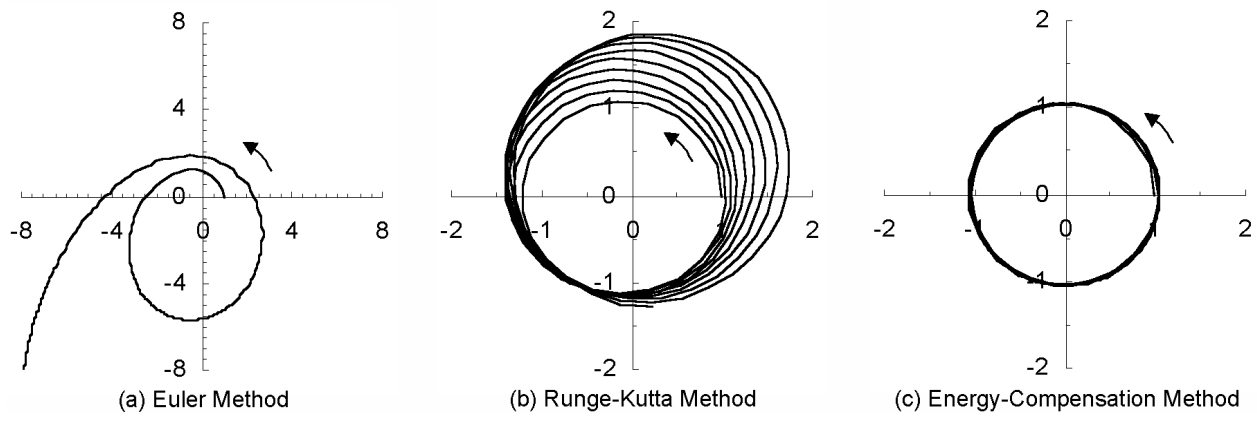

Fig. 5 Description of uniform circular motion

interval of motion. The direction of the ion velocity vector is not changed, but its length is adjusted to satisfy Eq. 4. As shown in Fig. 5c, compensation in this way yields the best numerical simulation for the uniform circular motion problem. This method is also preferred over Runge-Kutta not only because error accumulation is reduced via compensation but also because it requires fewer calculation steps and is, therefore, faster and more efficient.
It is noted that the Symplectic method[10] developed in 1990's is also conservative and efficient. In the present case, however, a preliminary feasibility study indicated it was unsuitable because of the large potential differences involved.

Pre-sheath Definition
As suggested previously, results obtained from optics simulations are strongly dependent on the shape of the ion extraction surface. In this simulation, a simple approach that recognizes a plasma consisting of ions and electrons in equilibrium exists upstream of an ion emitting sheath surface is used. The basic concept applied is suggested schematically in Fig. 6. It is assumed that the extreme left point, which is far upstream of the screen grid, is maintained at the discharge chamber plasma potential (ϕ_p) and that the potential of the other points as determined from the solution of the LaPlace equation are as shown in Fig. 6(a). As ions are injected from the extreme left (plasma) plane the potential of the points determined using Poisson's equation (Eq. 1) will rise above ϕ_p as shown in Fig. 6(b). If the calculated potential is over plasma space potential as shown in Fig. 6(c) it is argued that the higher potentials draw electrons (negative charges) from the adjoining plasma to maintain equilibrium. This causes the potentials to drop back to ϕ_p as suggested in Fig. 6(d). The mesh-point at ϕ_p which is furthest downstream is called the "plasma-internal-point," and the boundary connecting these points is called the "pre-sheath" in this study. Ions are extracted randomly from this pre-sheath with an initial velocity determined by the Bohm condition. The process of computing the pre-sheath location and shape is repeated using electrical potentials determined from the subsequent iteration of field calculations with ions being emitted from the pre-sheath. The iteration process under which the pre-sheath surface evolves and is coupled to the ion beam formation and acceleration processes is summarized in Fig. 7.
In a preliminary study, it was determined that the position and shape of the pre-sheath surface was independent of the distance between the initial upstream boundary and the screen grid (*i.e.* the line segment OA shown in Fig. 3), if this distance was greater than 1.5 times the radius OA.

Description of Charge-Exchange Phenomena
The charge-exchange reaction describes a collision between a fast ion and a slow neutral in accordance with the following equation:

$$A^{+}_{fast} + A_{slow} \rightarrow A^{+}_{slow} + A_{fast}$$

The charge-exchange reaction rate (dn_c / dt) of each cell (surrounded by eight mesh-points) is calculated using the number density of neutral particles in the cell (n_n), the number density of ions in the cell (n_i), the mean velocity of the ions in the cell (v_i) and the cross-section for the reaction [$\sigma_c(v_i)$] as follows:

$$\frac{dn_c}{dt} = n_n n_i v_i \sigma_c(v) \qquad (5)$$

The number density of neutrals, is determined using

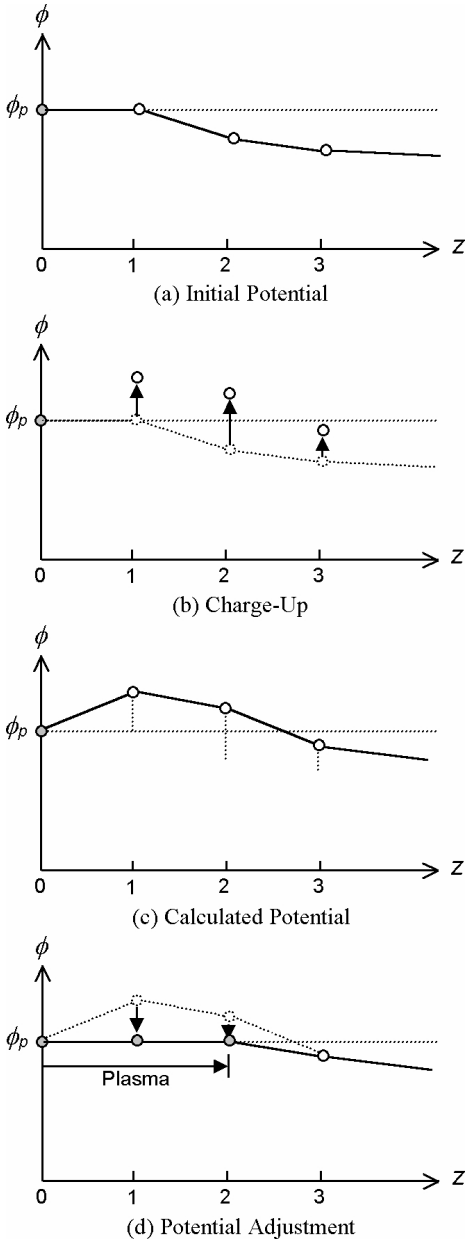

Fig. 6 Schematic of pre-sheath definition

conductance values for the grids and assuming, radially uniform free-molecular flow. Each charge-exchange ion is placed at the center-point of the cell in which it is produced and then moved to a boundary via the electrical field using the Euler method modified to include energy-compensation. The influence of charge-exchange ions on the intra-grid potentials is neglected.

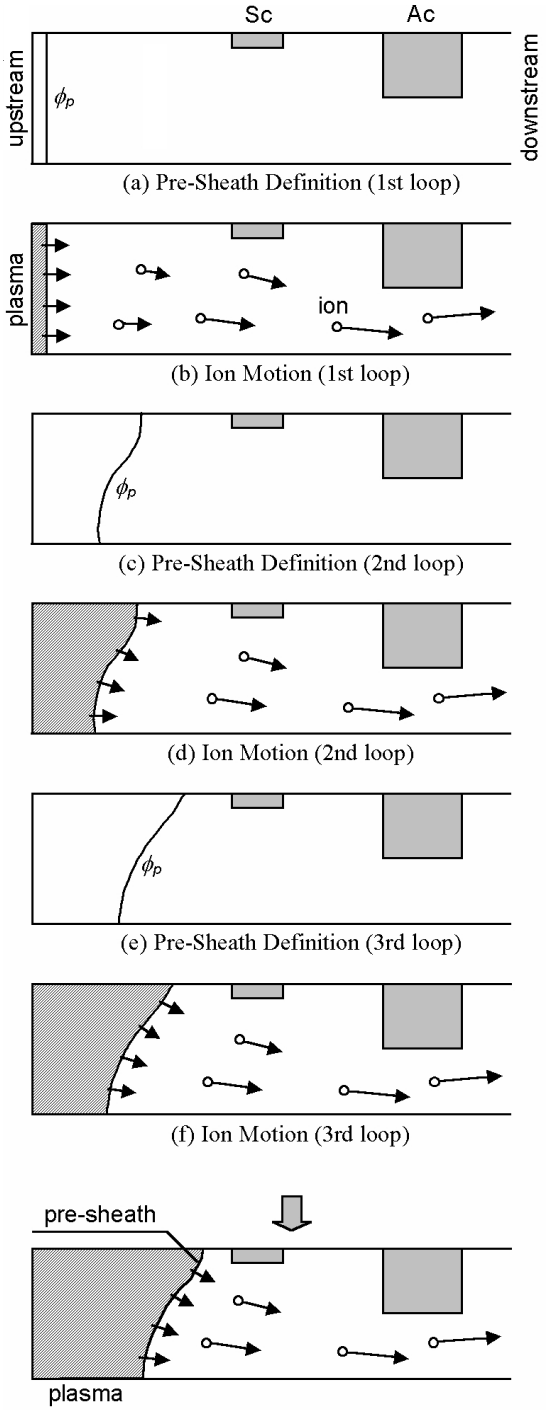

(a) Pre-Sheath Definition (1st loop)

(b) Ion Motion (1st loop)

(c) Pre-Sheath Definition (2nd loop)

(d) Ion Motion (2nd loop)

(e) Pre-Sheath Definition (3rd loop)

(f) Ion Motion (3rd loop)

(g) Pre-Sheath Definition and Ion Motion (Final loop)

Fig. 7 Schematic of pre-sheath

High-speed Coding

This simulation is coded in Fortran77 using the similar object-orientation method. It requires the use of a large memory but it enables rapid, low cost modeling. In order to realize reasonable simulation times the "igx" code is typically run 14 times with 1000 ions to establish the nominal pre-sheath and potentials before it is run a final time with 10,000 ions to define the final conditions.

Optimization Method for Design

Vast Search Space

The situation is made worse by the fact that many single-point design cases would have to be simulated to arrive at a final grid system design optimized for a particular mission. Even with expected increases in calculation speeds for conventional simulations are not expected to improve this situation because the number of design parameters (e.g. voltages and dimensions) that must be considered to optimize a grid system design necessitates a huge number of calculations. If it is assumed, for example, that a case can be simulated in one minute and 10 values are to be considered per parameter, the examination of 4 design parameters requires 10^4 minutes (~ 1 week) and examination of 6 parameters requires 10^6 minutes (~ 2 years). These estimates clearly demonstrate that the search space is too vast to allow a full simulation for all design parameters. In order for numerical codes to become more cost effective optimization tools, it seems obvious that a more efficient way of making large numbers of parametric calculations must be found.

Genetic Algorithm

A genetic algorithm[11-12] involves a kind of natural selection (Darwinian) process which employs genetic concepts and language and evolutionary theory. This algorithm is one in which the living specie is transposed into a collection of analytical parameters and the biological environment is transposed into an analytical environment. The level of adaptation of the species within a given environment corresponds to the optimization of a system through a fitness value that may have constraints imposed upon it. In a genetic algorithm, each analytical parameter is called a "gene," and by genetic analogy a parameter set is called a "chromosome". Moreover, the group of chromosomes that describe the collective system is called a "population." In a general genetic algorithm, a gene consists of several binary bits, and a chromosome has several genes. An analysis parameter set or chromosome is evolved through the sequence of processes: Initialization, Encoding, Evaluation and Repopulation (reproduction, crossover and mutation). The details of this method are discussed in a previous

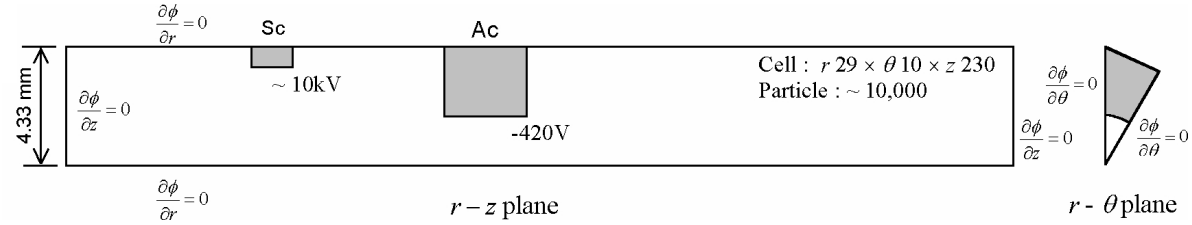

Fig. 8 HiIsp-IT grid system used for evaluation of code

paper[13]. In this work, it was confirmed that the genetic algorithm approach can be applied to search a huge multi-parameter space and identify gross, critical features of design.

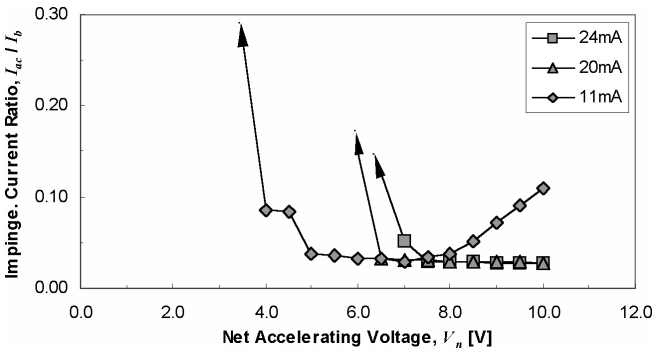

(a) Experiment

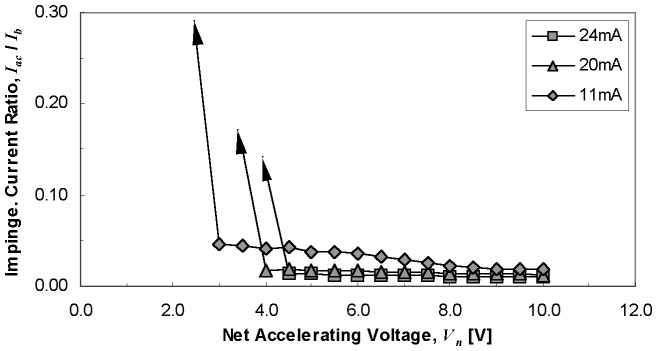

(b) OPT code simulation

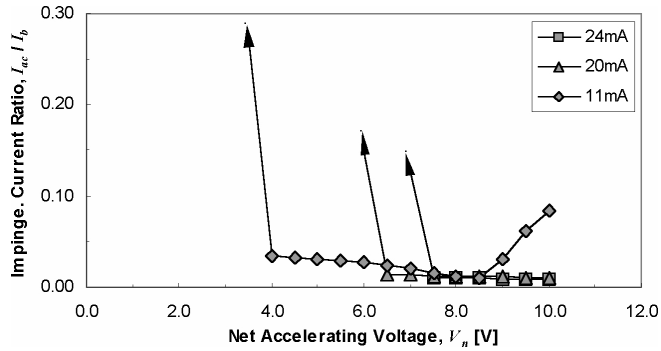

(c) "igx" code simulation

Fig. 9 Impingement current comparisons

Results and Discussion

Evaluation of Code

[Model] : Initial simulation runs carried out to evaluate the codes were performed on the two-grid HiIsp-IT systems shown to scale with boundary conditions and grid potentials in Fig. 8. The node distance used was 0.149 mm. There is a large gap between the screen and accelerating grids (5.5 mm) to prevent electrical breakdown. The screen grid is relatively thick (1.5 mm) because a thin grid yielded a high accelerating grid impingement current (I_{ac}) under some operating conditions. The accelerating grid is thick (3 mm) and has a small aperture diameter (3.5 mm) compared to that of the screen grid (7 mm) to assure a long life. Simulations were performed using both codes on an 800 MHz personal computer. Experimental results[14] obtained on a grid set with nineteen aperture pairs having the dimensions associated with Fig. 8 were available so they could be compared to simulation results. Krypton propellant flowing at a rate of 60 mA eq. is used in all cases.

[Impingement Current] : An example of comparative results obtained from this study are shown in Fig. 9. The experimental data shown were obtained by establishing one of the beam currents and measuring the impingement current as the screen grid voltage was varied. The plots show the variation in impingement to beam current ratio (I_{ac} / I_b) with net accelerating voltage (V_n). It is clear from a comparison of Figs. 9(a) and 9(b) that the results from the conventional code (OPT) do not agree well with experimental data in this case. On the other hand, a comparison of Figs. 9(a) and 9(c) shows that the "igx" code yields results that agree with the experimental data. This agreement was also confirmed in the other simulation cases.

[Pre-sheath Form] : Figure 10 shows the code prediction of changes in pre-sheath position and shape as net accelerating voltage is varied when the beam current is 11 mA. As net accelerating voltage is increased this figure shows the pre-sheath becomes increasingly concave upstream and further from the screen grid. On the other hand, the sheath is convex (ballooned downstream) and positioned further downstream in the lowest voltage case. These results are consistent with crossover impingement at higher voltages and perveance-limited impingement when the

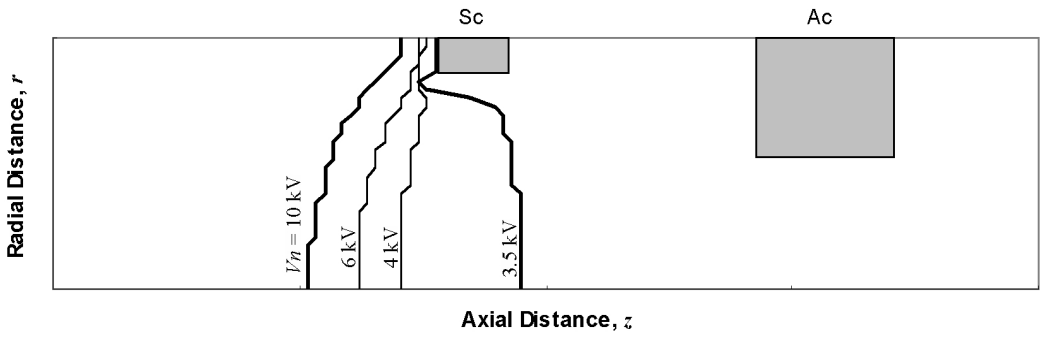

Fig. 10 Pre-sheath configurations

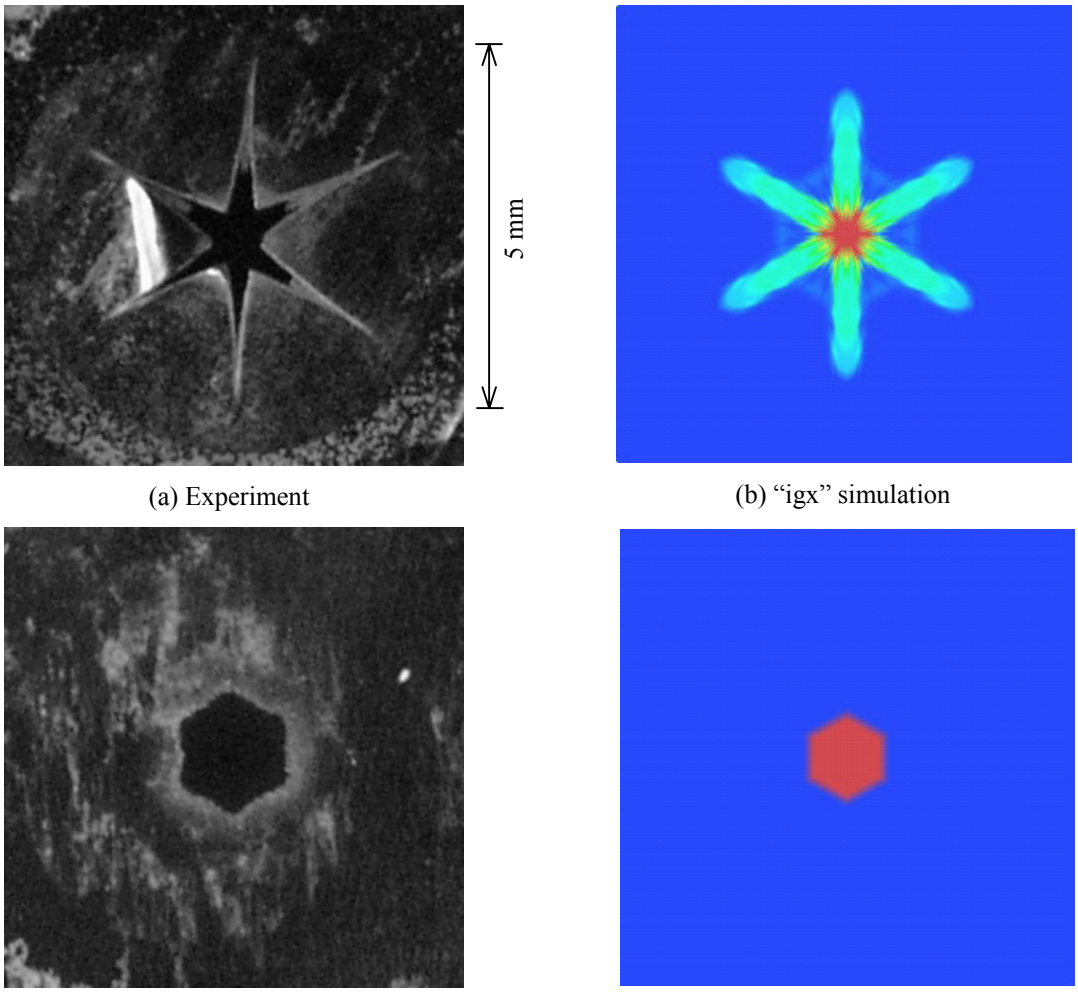

(a) Experiment (b) "igx" simulation

(c) Experiment (d) "igx" simulation

Fig. 11 Cross-section shapes (a, b : star-shaped-pattern, c, d : hexagonal-pattern)

voltage is lowest. These impingement phenomena were confirmed in our experiments.

[Beamlet Cross-section Shapes] : The patterns in Figs. 11(a) and 11(c) are experimental results which were produced by spot welding a 13 μm thick Ta foil to the upstream surface of the acceleration grid and then allowing the foil to be eroded by ion beamlets that were being extracted. Figures 11(b) and 11(d) show the cross-section form derived from the "igx" simulation. These results indicate that the results from "igx" simulation are in good agreement with the experimental data (star-shaped and hexagonal patterns).

[Calculation Speed] : Simulation using the "igx" code required 6 ~ 10 minutes per case for the above simulation (hereafter called the "standard-simulation"), and 5 ~ 7 seconds for the rough-simulation, on a 800 MHz personal computer. The rough-simulation results exhibit ~ 10% error compared to the "standard-simulation" results In addition, this simulation used 5 ~ 40 MB of memory.
[Evaluation] : The above results and estimations suggest that the "igx" code simulation is better suited to the analysis and design of HiIsp-IT grid systems because of its agreement and speed.

Discussion of Optimization Method for Design
[Coupling with Genetics Algorithm] : The 21-bit chromosome used in this simulation is composed of 5 genes. The values of genes and fixed quantities were set as represented in Table 1. The search space associated with the chromosome is then 2^{21} (~10^6). The "igx" simulation, which was described previously, is incorporated into the genetic algorithm in the evaluation module. This module ("igx") calculates and optimizes on the following a fitness value:

$$fv = (ft \times cr)^{100} \qquad (6)$$

Table 1 Values of genes and fixed quantities

			Value	cf	
Total Beam Current I_b [mA]			12, 18, 24, 30, 36, 42	Target (6)	
Sc.-grid	Potential	V_{sc} [V]	10,000	-	
	Diameter	D_{sc} [mm]	7.0	-	
	Thickness	t_{sc} [mm]	0.25 ~ 4.00 (step 0.25)	gene_1 (4-bits)	Chromosome
Grid-gap		L_g [mm]	4.50 ~ 8.25 (step 0.25)	gene_2 (4-bits)	
Ac.-grid	Potential	V_{ac} [V]	(-) 200 ~ 510 (step 10)	gene_3 (5-bits)	
	Diameter	D_{ac} [mm]	3.50 ~ 7.00 (step 0.50)	gene_4 (4-bits)	
	Thickness	t_{ac} [mm]	0.50 ~ 4.25 (step 0.25)	gene_5 (4-bits)	

In this value, *ft* and *cr* are the thrust factor and the beam current ratio. These are calculated by the following equations:

$$ft = \sum \left(\frac{v_r}{\sqrt{{v_z}^2 + {v_r}^2}} \right) \qquad (7)$$

$$cr = \frac{(I_b - I_{CX})}{I_b} \qquad (8)$$

In these equations, v_r, v_z, I_{CX} and I_b are the radial ion velocity; the axial ion velocity; the charge-exchange current which impinges on the accelerator grid; and the beam current. The exponent 100 was applied in Eq. (6), 100, to amplify differences between fitness values. In addition, the minimum potential (*potcl*) on the center axis was calculated and checked. If the minimum potential insufficient to prevent beam plasma electron backstreaming ($potcl > -T_e$), the fitness value was set zero. In this study, the electron temperature (T_e) was 5 eV. Moreover, the fitness value of the chromosome that has the highest value in each generation was stored and no recalculation was done for that chromosome.
The chromosomes are evolved using the algorithm and evaluated by the "igx" simulation until the grid system parameters have been optimized. Moreover, the population is composed of 100 chromosomes in each generation, and the evolution is terminated at the 100th generation.
[Typical Results] : Figure 12 shows the typical grid system design parameters optimized using the genetic algorithm. This figure indicates that the grid gap (l_g) and the screen grid thickness (t_{sc}) are large at lower beam currents and small at greater beam currents. It is

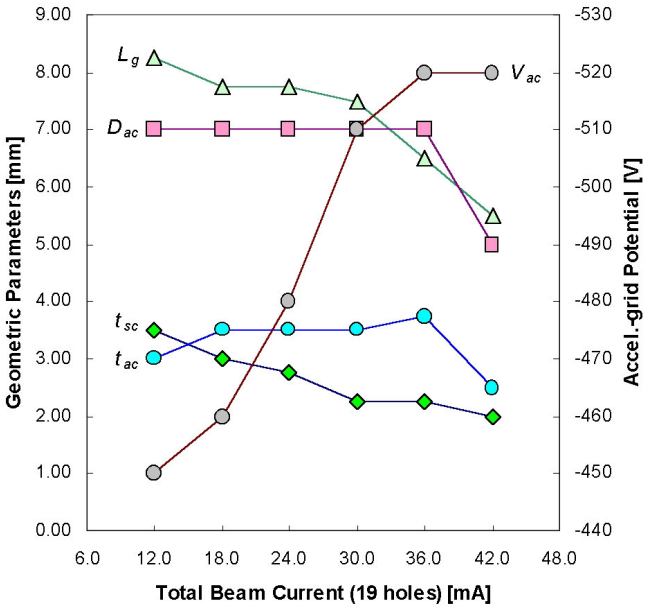

Fig. 12 Optimized design parameters

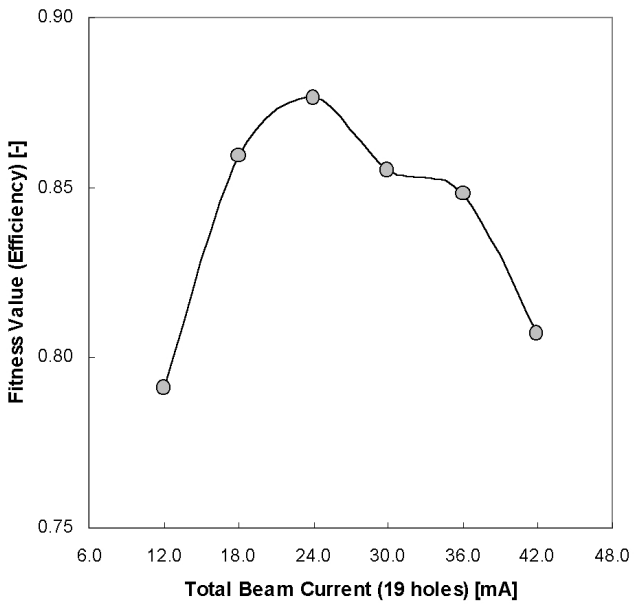

Fig. 13 Fitness value

likely that these limits are associated with the onset of space charge limited currents. This figure also indicates that the applied potential and thickness of acceleration grid (V_{ac} and t_{ac}) are low and small in lower beam current case and high and large in the higher beam current case. It appears that these are optimized to assure there is no electron back streaming. Moreover, the figure also indicates that the optimized diameter of acceleration grid is the maximum ($D_{ac} = 7.0$ mm $= D_{sc}$). It seems that a large value of D_{ac} yields a low charge-exchange current by reducing the intra-grid neutral density. However, it is likely that this analysis should involve simulation of both grid and discharge chamber phenomena this neutral density is affected by both. Figure 13 shows the relationship between the fitness value and the total beam current. As shown in this figure, the fitness value for $I_b = 1.263$ mA/hole (= 24 mA/19 holes) is the highest. It is likely that the ion is extracted with the highest efficiency under the conditions: $D_{sc} = 7.0$ mm and the hole center-to-center distance = 7.5 mm.

These results are based on the assumption that the highest fitness value as expressed in Eq. (6) yields best grid system parameter set. Other fitness values will be of greater interest for many missions.

[Searching Efficiency] : It was determined that the evolution was completed by 10~80th generation. This suggests that only 10^4 (~80×100) calculations are required to optimize the grid system parameters. Because this is small compared to the full search space of 2^{21} (~10^6), one can conclude that the genetic algorithm is very efficient. Moreover, it was found that the execution time required to optimize a system with 100-chromosomes over 100-generations with an 800 MHz personal computer was only about a half day. This corresponds to an average "igx" simulation time of about 4.5 sec. per chromosome.

Concluding Remarks

(1) The developed three-dimensional particle simulation code "igx" which uses an energy compensation method, a simplified pre-sheath definition method and high-speed coding yields results that are in good agreement with experiment data: impingement currents and beamlet cross-sectional shapes.
(2) The genetic algorithm approach can be applied to search a huge multi-parameter space and identify gross, critical features of grid system design.
(3) More detailed analysis, optimization method and discussion of grid design options for HiIsp-IT grid systems is needed.

Acknowledgement

Partial financial support for this work was provided under Research Grant NAG3-1801 by the NASA Glenn Research Center. This support is gratefully acknowledged.

References

[1] Whealton, J. H., McGaffey, R. W. and Stirling, W. L., "Ion beam extraction from a plasma with aberration reduction by method of mutual exclusion," Journal of Applied Physics, Vol. 52, No. 6, 1981

[2] Personal Communication with Dr. Yukio Hayakawa (National Aerospace Laboratory, Japan)

[3] Free, B., Owens, J. R. and Wilbur, P., "Variations of triple-grid geometory and potentials to alleviate accel grid erosion," 22nd International Electric Propulsion Conference, IEPC-91-120, Italy, 1991

[4] Nakano, M. and Arakawa, Y., "Ion Thruster Lifetime Estimation and Modeling Using Computer Simulation," 26th International Electric Propulsion Conference, IEPC-99-145, Japan, 1999

[5] Okawa, Y. and Takegahara, H., "Particle Simulation on Ion Beam Extraction Phenomena in an Ion Thruster," 26th International Electric Propulsion Conference, IEPC-99-146, Japan, 1999

[6] Muravlev, V. A. and Shagayda, A. A., "Numerical Modeling of Extraction Systems in Ion Thrusters," 26th International Electric Propulsion Conference, IEPC-99-162, Japan, 1999

[7] Personal Communication with Professor Yoshihiro Arakawa (University of Tokyo, Japan) and Dr. Masakastu Nakano (National Aerospace Laboratory, Japan)

[8] Nakayama, Y. and Wilbur, P. J., "Numerical Simulation of Ion Beam Optics for Many-grid Systems", 37th Joint Propulsion Conference, AIAA 2001-3782, Salt Lake City, UT, 2001

[9] Birdsall, C. K. and Langdon, A. B., *Plasma Physics via Computer Simulation*, McGraw-Hill, 1985

[10] Giaquinta, M., Shatah, J. and Varadhan, S. R. S., *Differential Equations: La Pietra 1996*, Proceedings of Symposia in Pure Mathematics, Vol. 65, 1996

[11] Holland, J. H., *Adaptation in Natural and Artificial Systems*, University of Michigan Press, 1975

[12] Winter, G., Periaux, J., Galan, M. and Cuesta, P., *Genetic Algorithms in Engineering and Computer Science*, John Wiley & Sons, 1995

[13] Nakayama, Y. and Wilbur, P. J., "The Feasibility of a Genetic-Algorithm-Based Ion Thruster Design Code", 37th Joint Propulsion Conference, AIAA 2001-3786, Salt Lake City, UT, 2001

[14] Wilbur. P.J, Miller J, Farnell, C and Rawlin, V.K., "A Study of High Specific Impulse Ion Thruster Optics," 27th International Electric Propulsion Conference, IEPC-01-098, Pasadena, CA, 2001